ISME Communications, 2024, 4(1), ycae070
https://doi.org/10.1093/ismeco/ycae070
Advance access publication: 8 May 2024
Original Article

pH selects for distinct N_2O-reducing microbiomes in tropical soil microcosms

Yanchen Sun[1,2,8], Yongchao Yin[2,3,9], Guang He[4], Gyuhyon Cha[5], Héctor L. Ayala-del-Río[6], Grizelle González[7], Konstantinos T. Konstantinidis[5], Frank E. Löffler[1,2,3,4,*]

[1]Department of Civil and Environmental Engineering, University of Tennessee, Knoxville, Knoxville, TN 37996, United States
[2]Center for Environmental Biotechnology, University of Tennessee, Knoxville, Knoxville, TN 37996, United States
[3]Department of Microbiology, University of Tennessee, Knoxville, Knoxville, TN 37996, United States
[4]Department of Biosystems Engineering and Soil Science, University of Tennessee, Knoxville, Knoxville, TN 37996, United States
[5]School of Civil and Environmental Engineering, Georgia Institute of Technology, Atlanta, GA 30332, United States
[6]Department of Biology, University of Puerto Rico at Humacao, Humacao 00792, Puerto Rico
[7]USDA Forest Service, International Institute of Tropical Forestry, San Juan 00926, Puerto Rico
[8]Present address: Department of Marine Chemistry and Geochemistry, Woods Hole Oceanographic Institution, Woods Hole, MA 02543, United States
[9]Present address: Department of Biology, Antimicrobial Discovery Center, Northeastern University, Boston, MA 02148, United States

*Corresponding author: Frank E. Löffler, Department of Civil and Environmental Engineering, University of Tennessee, 325 John D. Tickle Building, 851 Neyland Drive, Knoxville, TN 37996, United States. Email: frank.loeffler@utk.edu

Abstract

Nitrous oxide (N_2O), a greenhouse gas with ozone destruction potential, is mitigated by the microbial reduction to dinitrogen catalyzed by N_2O reductase (NosZ). Bacteria with NosZ activity have been studied at circumneutral pH but the microbiology of low pH N_2O reduction has remained elusive. Acidic (pH < 5) tropical forest soils were collected in the Luquillo Experimental Forest in Puerto Rico, and microcosms maintained with low (0.02 mM) and high (2 mM) N_2O assessed N_2O reduction at pH 4.5 and 7.3. All microcosms consumed N_2O, with lag times of up to 7 months observed in microcosms with 2 mM N_2O. Comparative metagenome analysis revealed that *Rhodocyclaceae* dominated in circumneutral microcosms under both N_2O feeding regimes. At pH 4.5, *Peptococcaceae* dominated in high-N_2O, and *Hyphomicrobiaceae* in low-N_2O microcosms. Seventeen high-quality metagenome-assembled genomes (MAGs) recovered from the N_2O-reducing microcosms harbored *nos* operons, with all eight MAGs derived from acidic microcosms carrying the Clade II type *nosZ* and lacking nitrite reductase genes (*nirS/K*). Five of the eight MAGs recovered from pH 4.5 microcosms represent novel taxa indicating an unexplored N_2O-reducing diversity exists in acidic tropical soils. A survey of pH 3.5–5.7 soil metagenome datasets revealed that *nosZ* genes commonly occur, suggesting broad distribution of N_2O reduction potential in acidic soils.

Keywords: nitrous oxide (N_2O), greenhouse gas, non-denitrifying N_2O reducers, acidic soils, low pH N_2O reduction, Clade II N_2O reductase (NosZ)

Introduction

Nitrous oxide (N_2O) is a long-lived ozone-depleting greenhouse gas with a global warming potential far exceeding that of the equivalent amount of CO_2 [1, 2]. The global atmospheric N_2O concentration has increased from 270 parts per billion (ppb) in 1750 to 331 ppb in 2018 [3]. During the 2007 to 2016 time period, the net global atmospheric N_2O increase was estimated at 4.3 Tg N $year^{-1}$ [4], indicating that N_2O sources outpace N_2O sinks. Major sources of N_2O include denitrification ($NO_3^-/NO_2^- \rightarrow N_2O$) [5] and chemodenitrification [6], with additional N_2O released from nitrification ($NH_4^+ \rightarrow NO_3^-$) [7] and dissimilatory nitrate reduction to ammonium ($NO_3^-/NO_2^- \rightarrow NH_4^+$) [8]. Compared to multiple sources of N_2O, its consumption catalyzed by N_2O reductase (NosZ) is the major natural biotic sink.

Canonical, complete denitrifiers possess the *nos* operon and can synthesize NosZ responsible for N_2O reduction to dinitrogen (N_2), the latter a gas without warming potential. Genomic analyses distinguished two types of *nos* operons with distinct *nosZ*: Clade I *nosZ* generally associated with canonical denitrifying bacteria and Clade II *nosZ* often found on genomes lacking the denitrification biomarker genes *nirS* or *nirK* [9–11]. Subsequent studies reported that Clade II *nosZ* are generally more abundant and diverse in soils than Clade I *nosZ* [12, 13], suggesting N_2O reduction potential outside the group of complete denitrifiers. Kinetic studies using axenic bacterial cultures demonstrated that Clade II N_2O reducers exhibit higher affinities to N_2O and growth yields than their N_2O-reducing Clade I counterparts [14], suggesting Clade II reducers capture energy during growth with N_2O as electron acceptor more efficiently. Environmental factors, including pH, temperature, O_2 levels, substrate availability, and NO_3^-/NO_2^- levels are known to affect N_2O reduction [15–17]. The final reduction step ($N_2O \rightarrow N_2$) catalyzed by NosZ was found particularly sensitive to pH,

Received: 29 November 2023. **Revised:** 27 April 2024. **Accepted:** 7 May 2024

explaining N_2O emissions from acidic environments [18, 19]. Expression studies suggested posttranscriptional interference at low pH, with the NosZ remaining in the catalytically inactive apoform, a possible reason for the observed decline in NosZ activity under acidic conditions [18, 20].

Natural soils are the dominant source of N_2O (~5.6 Tg N_2O-N $year^{-1}$), accounting for ~33% of global N_2O emissions [4], with tropical forest soils contributing ~1.34 Tg N_2O-N $year^{-1}$ [21]. Tropical soils were reported to emit N_2O at a rate of 0.1 ± 0.04 g N_2O-N m^{-2} $year^{-1}$, which is about 50% above the average rate of global soil N_2O emissions [22]. The large contribution of tropical soils to N_2O emissions has been explained by high N_2 fixation activity and generally acidic soil pH [23–25]. N_2O production can be sporadic suggesting that fluxes and concentrations of N_2O can vary substantially both over temporal and spatial scales [26]. A comparative metagenomic study found similar relative abundances of *nosZ* sequences in acidic tropical and circumneutral temperate soils [23]. Apparently, acidic tropical soil environments have the metabolic potential to reduce N_2O, a hypothesis supported by isotopic measurements that revealed biotic reduction of N_2O in acidic tropical forest soils [24]. Although some evidence for N_2O reduction under acidic conditions exists, the consensus backed by laboratory observations is that N_2O reduction is negligible at acidic pH [18, 20, 27, 28].

To reconcile existing inconsistencies between field measurements and laboratory studies, and to explore the impacts of pH and N_2O concentration on N_2O-reducing microorganisms, acidic (pH 4.4–5.0) soil samples were collected in the Luquillo Experimental Forest (LEF) in Puerto Rico. A series of microcosms explored the impact of pH (i.e. 4.5 versus circumneutral) and N_2O concentrations (i.e. 0.02 and 2 mM) on N_2O reduction. Metagenome analyses indicate that both pH and N_2O concentration select for distinct N_2O-reducing microbiomes and suggest widespread distribution of N_2O reduction potential across various acidic soil ecosystems.

Materials and methods

Soil collection

Soil samples were collected from four locations (5–20 cm depth) in the LEF in Puerto Rico, including the El Verde tabonuco forest (EV, 453 m above mean sea level [MSL]), the Palm Nido palm forest (PN, 634 m MSL), the Pico del Este elfin forest (PE, 953 m MSL), and the Sabana tabonuco forest (S, 265 m MSL) (Supplementary Fig. S1). The soil materials were transferred to sterile Whirl-Pak bags, placed at 4°C, and manually homogenized prior to microcosm setup. Detailed descriptions of the LEF can be found elsewhere [29, 30], and physicochemical properties of the soil samples are presented in Supplementary Table S1.

Soil microcosms

Completely synthetic, reduced (0.2 mM L-cysteine) mineral salt medium was prepared following established protocols [31]. In the pH 4.5 medium, 50 mM potassium dihydrogen phosphate replaced the 30 mM bicarbonate buffer used in the pH 7.3 medium [32]. The pH was adjusted with CO_2 (pH 7.3 medium) or with 4 M hydrochloric acid (pH 4.5 medium). $CuCl_2$ (17 μM) and the Wolin vitamin mix were added from concentrated stock solutions to individual 160 mL glass serum bottles after autoclaving [32].

Inside a glove box (Coy Laboratory Products, Grass Lake, MI) filled with 97% N_2 and 3% H_2, 2 g (wet weight) of homogenized soil material was aseptically transferred to sterile glass serum bottles containing 100 ml of medium using stainless-steel spatulas. The serum bottles were immediately resealed with sterile butyl rubber stoppers, crimped with aluminum caps, and removed from the glove box. Lactate (5 mM) was added to each serum bottle from a 1 M stock solution by syringe and replenished four times over the 15-month incubation period. Two replicate series of microcosms were established at pH 4.5 and at pH 7.3 with duplicate pH 4.5 microcosms (Supplementary Fig. S1). Plastic syringes (Becton, Dickinson and Company, Franklin Lakes, NJ) with 25-gauge needles (Becton, Dickinson and Company) were used to add 0.1 ml (4.17 μmol, 0.02 mM aqueous N_2O) and 10 ml (416.7 μmol, 2 mM aqueous N_2O) of undiluted N_2O gas to the incubation vessels. N_2O was periodically analyzed by gas chromatography (GC) as described [32] and replenished when consumed. All bottles were incubated at 30°C under static conditions for 15 months. Negative controls included heat-killed (autoclaved) replicates and microcosms without N_2O but with lactate at pH 4.5 for each soil sample.

Analytical procedures

N_2O was analyzed with an Agilent 3000A Micro-GC (Agilent, CA) equipped with a thermal conductivity detector and a Plot Q column [14]. The limit of detection was 50 ppmv of N_2O with signal-to-noise ratio of 3:1. The injector and column temperatures were set to 100°C and 50°C, respectively, and the column pressure was set to 25 psi. For each measurement, a 0.1 ml headspace sample was withdrawn from the microcosm and manually injected into the Micro-GC. Aqueous N_2O concentrations were calculated from the headspace concentration using a dimensionless Henry's constant for N_2O at 20°C of 1.68 based on the equation $C_{aq} = C_g/H_{cc}$ [33]. C_{aq} and C_g are the aqueous N_2O and the headspace N_2O concentrations (μM), respectively, and H_{cc} is the dimensionless Henry's constant. The total amount of N_2O was calculated as the sum of N_2O in the headspace and the aqueous phase.

DNA extraction and metagenome sequencing

When about half of the final N_2O amendment had been consumed, the microcosms were shaken, and 5 ml suspension samples were collected with 5-ml plastic syringes equipped with 18-gauge needles. DNA for shotgun metagenome sequencing was extracted with the DNeasy PowerSoil kit (Qiagen, Hilden, Germany) according to the manufacturer's instructions. DNA concentrations were determined using the Qubit fluorometer (Life Technologies, Carlsbad, CA). Metagenome sequencing was performed at the Institute for Genome Sciences at the University of Maryland using the Novaseq 6000 platform (Illumina, San Diego, CA) to generate 48 to 73 million reads with 150-bp read length per sample (Supplementary Table S2). Replicate high- and low-N_2O pH 4.5 microcosms showed similar N_2O reduction performance, and a single microcosm per treatment was randomly selected for metagenome sequencing.

Bioinformatic analysis

The metagenomes of the four original soils had been sequenced previously [23], and were downloaded from European Nucleotide Archive under project PRJEB26500. The raw reads of the original soils and of the 16 N_2O-reducing microcosms were trimmed with Trimmomatic v0.39 using default parameters [34]. Subsequent assembly was performed using IDBA-UD v1.1.3 [35], and only contigs longer than 1000 bp were included in downstream analyses. Contigs were binned using MaxBin2 v2.2.4 with default settings to recover individual metagenome-assembled genomes (MAGs) [36]. MAGs were dereplicated with dRep using default

parameters [37] and checked for completeness and contamination using CheckM v1.0.18 [38]. The resulting MAGs were evaluated for their intrapopulation diversity and sequence discreteness using fragment recruitment analysis scripts available through the Enveomics collection [39]. The coverage of each MAG in each metagenome was calculated by estimating sequencing depth at each position using Bowtie 2 [40] with default settings for read mapping. In addition, BEDTools [41] was used to calculate the average of the central 80% of the distribution, which removes the highest and lowest 10% of outlier positions in terms of coverage (i.e. the truncated average depth [TAD80]). TAD80 is a conservative metric that produces no false-positive results [42]. TAD80 values were normalized by the genome equivalent of the corresponding metagenome to determine the relative abundance. The genome equivalents of each metagenomic dataset were obtained using the MicrobeCensus package [43].

Metagenomic community profiling

GraftM v0.13.1 was used to extract 16S rRNA gene fragments from the trimmed metagenomic datasets for classification using the Greengenes database (release 13_8) at the 97% nucleotide identity level [44, 45]. The relative abundance of operational taxonomic units (OTUs) was calculated based on the number of reads assigned to each OTU. Community profiling was based on OTU taxonomic assignments at the phylum, family, and genus levels.

Identification of *nosZ* genes

ROCker was used to identify metagenomic reads carrying *nosZ* [46]. Briefly, trimmed short reads were used as the query for BLASTX (Diamond v0.9.14.115) searches against the corresponding ROCker protein database representing the target gene [47]. The matching sequences were then filtered using the ROCker compiled models available through the Enveomics collection (http://enve-omics.ce.gatech.edu/) [39]. The abundances of target genes (i.e. Clade I and Clade II *nosZ*) were determined by calculating the ratio between normalized target reads (counts divided by the median protein length) and the genome equivalents [48]. Reference *nosZ* genes were also searched against the assemblies and MAGs using precompiled hidden Markov models obtained from FunGene and HMMer [49, 50]. Hits with an identity value of 100% were filtered based on the NosZ sequences in the reference database [23].

NosZ phylogeny

NosZ reference sequences were aligned with ClustaloΩ using default settings [51]. The alignment was used to build a maximum likelihood reference tree in RAxML V8.2.12 with "-f a" algorithm, gamma parameter optimization, and a general time reversible model option [52]. ROCker identified reads carrying *nosZ*, which were translated to protein sequences using MetaGeneMark [53]. The translated sequences were added to the NosZ reference protein alignment using MAFFT and the "addfragments" option [54], and the new alignment placed in the NosZ reference phylogenetic tree using RAxML EPA algorithm (–f v option). The generated jplace file was processed using an in-house script (available through http://enve-omics.ce.gatech.edu/) for visualization in iTOL [55]. Detected NosZ proteins in the assemblies and MAGs were manually curated, added to the phylogenetic trees, and visualized as described above.

Taxonomic assignment, functional annotation, and comparative genomics

Taxonomic assignments of MAGs with >75% completeness and < 5% contamination used the GTDB-Tk v0.1.4 tool [56] of the Genome Taxonomy Database (GTDB, http://gtdb.ecogenomic.org) version R202 [57]. At this level of completeness, genes not assembled in a MAG likely represent mobile and hypothetical genes, rather than characterized functional genes [58]. Protein-coding sequences were predicted using Prodigal v2.6.3 [59], and assigned Kyoto Encyclopedia of Genes and Genomes (KEGG) orthologs using KofamScan v1.3.0 against Hidden Markov model (HMM) profiles from the KEGG database (release February 2021) [60]. The completeness of various metabolic pathways was assessed using KEGG-Decoder v1.32.0 [61], and pathways of interest (e.g. nitrogen cycling, lactate and hydrogen metabolism, copper transport) were manually selected from the KEGG-Decoder results. Average nucleotide identity and average amino acid identity (AAI) between high-quality MAGs and genomes of phylogenetically related bacteria were calculated with MiGA (http://microbial-genomes.org/). Phylogenetic trees were created using FastTree 2.1.8 (WAG+GAMMA models) with a concatenated alignment of 120 bacterial and 122 archaeal conserved marker genes [62] and visualized in iTOL [55].

N_2O reduction potential in acidic soils

From MAGs and contigs from acidic N_2O-reducing microcosms, 33 near full-length NosZ sequences were recovered (Supplementary Figs S2 and S3), and dereplication yielded eight unique NosZ sequences. A customized database was generated that comprised 14 NosZ, including six closely related sequences from the reference NosZ database. To identify *nosZ* genes recovered from acidic N_2O-reducing microcosms in various soil microbiomes, 35 available soil metagenome datasets derived from representative pH 3.5–7.5 environmental systems were downloaded from the European Nucleotide Archive (Supplementary Table S3) and subjected to BLASTX query using the customized NosZ database with a minimum identity value of 60% and an e-value of 1e-05. The normalization approach described above was used to calculate relative abundances based on *nosZ*-carrying metagenomic reads.

Statistics

Statistical analyses were performed using R version 4.0.2. Beta diversity was calculated using Bray–Curtis dissimilarity and visualized using the principal coordinate analysis (PCoA) plot in R with packages ggplot2 [63] and phyloseq [64]. Statistical differences in microbial communities among original soils, pH 4.5 microcosms, and pH 7.3 microcosms were determined using permutational multivariate analysis of variance (PERMANOVA) using the Adonis function in vegan with 999 permutations [65]. Heatmaps of annotation results of MAGs were generated using the R package pheatmap.

Results

N_2O reduction in tropical forest soil microcosms

N_2O consumption occurred with lag times of 1–2 weeks in pH 4.5 and pH 7.3 microcosms with low level of 0.02 mM N_2O. Longer lag times of up to 7 months were observed in microcosms with 2 mM N_2O under both pH conditions, but microcosms with high-level N_2O consumed substantially more N_2O over the 15-month incubation period (Supplementary Fig. S4 and

Supplementary Table S4). No N_2O loss occurred in autoclaved microcosms, indicating the acidic tropical forest soils harbor N_2O-reducing microorganisms. In addition, no N_2O was detected in control microcosms without N_2O amendment, indicating that N_2O formation from nitrogenous compounds in the medium or associated with the soil did not occur or was negligible.

Bacterial community composition

Following a 15-month incubation period and when the microcosms had consumed about half of the final N_2O feeding, DNA was extracted for metagenome sequencing. The overarching goal was to assess if the enrichment conditions selected for different N_2O-reducing taxa, rather than a fine-scale analysis of the overall community responses over the 15-month incubation. Therefore, single microcosms per treatment were subjected to metagenome sequencing. Totals of 5963 ± 2503 and $23\,399 \pm 15\,030$ sequences representing 16S rRNA genes were obtained from the original soil and the corresponding microcosm metagenome datasets, respectively, and yielded 903 16S rRNA gene-based OTUs (Supplementary Table S5). Rarefaction analysis suggested that the number of unique 16S rRNA genes approached saturation in most samples (Supplementary Fig. S5), and the number of OTUs detected in N_2O-reducing microcosms was lower than in the corresponding original soils. Beta diversity analysis using the 16 microcosm- and four original soil- [23] derived metagenomic datasets indicated distinct community compositions in response to pH and N_2O levels ($P < .01$, PERMANOVA) (Fig. 1A, Supplementary Table S6). PCoA revealed that ~55% of the total variability of OTUs observed in pH 4.5 and in circumneutral N_2O-reducing microcosms compared to the respective original soils was explained by pH and N_2O (Fig. 1A). Datasets acquired from same pH microcosms established with the four different soils clustered together indicating that pH shaped distinct microbial communities over the 15-month incubation period (Fig. 1). The majority of the 16S rRNA gene sequences derived from the original soils affiliated with the phyla *Proteobacteria*, *Actinobacteria*, *Verrucomicrobia*, *Planctomycetes*, and *Acidobacteria*, with a combined relative abundance exceeding 70% (Fig. 1B). Higher relative abundances of *Proteobacteria*, *Firmicutes*, *Chloroflexi*, and *Actinobacteria* were observed in the 16 N_2O-reducing microcosms relative to the original soil inoculum. Analysis at the family level showed that sequences representing *Peptococcaceae*, *Veillonellaceae*, *Clostridiaceae*, and *Hyphomicrobiaceae* increased in acidic microcosms, and sequences of *Rhodocyclaceae*, *Clostridiaceae*, *Hyphomicrobiaceae*, and *Ruminococcaceae* were more abundant in microcosms maintained at circumneutral pH compared to the original soils (Supplementary Fig. S6A). Based on the relative abundances of 16S rRNA gene sequences (highest observed values shown in parentheses), the genera *Desulfosporosinus* (45%), *Desulfomonile* (5%), *Rhodoplanes* (53%), *Azospira* (56%), and *Dechloromonas* (38%) increased in response to N_2O additions compared to the original soils (Supplementary Fig. S6B). At least some members of these genera comprise known N_2O-respiring species [9], suggesting that bacteria capable of using N_2O as an electron acceptor were enriched.

Phylogenetic distribution and relative abundance of Clade II versus Clade I *nosZ*

N_2O reduction is catalyzed by NosZ and *nosZ* gene abundances increased during enrichment with N_2O. The analysis of the metagenome datasets showed that Clade II *nosZ* sequences outnumbered Clade I *nosZ* gene sequences in the original soils and in the N_2O-reducing microcosms (except microcosm S_pH7.3_0.1) (Supplementary Fig. S7, Supplementary Table S7). Placing Clade II *nosZ* sequence reads extracted from the original soil metagenome datasets in the reference Clade II *nosZ* phylogenetic tree revealed affiliations with the genera *Anaeromyxobacter* and *Opitutus* (Fig. 2A). In contrast, the *nosZ* sequence reads observed in the acidic microcosms were assigned to the genera *Profundibacter*, *Desulfosporosinus*, and *Desulfomonile* (Fig. 2B and C). In microcosms maintained at pH 7.3, the majority of *nosZ* reads affiliated with the genera *Azospira*, *Dechloromonas*, and *Sulfuricella* (Fig. 2D and E), except for the EV soil microcosms with high level of N_2O, where *nosZ* sequences assigned to the genus *Desulfosporosinus* dominated. A comparative analysis of Clade II *nosZ* reads revealed that the microcosms maintained at pH 4.5 and at pH 7.3 developed distinct N_2O-reducing communities ($P < .01$, PERMANOVA) (Supplementary Fig. S8A). Taken together, these analyses suggest that bacteria with Clade II *nosZ* drive N_2O reduction in all tropical soil microcosms, and pH selects for distinct Clade II N_2O reducers (Fig. 2).

Most of the Clade I *nosZ* sequences could be assigned to the genus *Bradyrhizobium*, and a small number of reads affiliated with the genera *Methylocystis*, *Methylocella*, and *Janthinobacterium*, independent of the pH conditions or N_2O levels (Fig. 2F–J). Apparently, acidic versus circumneutral pH and low versus high N_2O levels did not select for distinct Clade I *nosZ* N_2O reducers. The PCoA supports that acidic pH and circumneutral pH conditions selected for similar Clade I N_2O reducers ($P > .05$, PERMANOVA) (Supplementary Fig. S8B).

Metagenome-assembled genomes

A non-redundant set of 17 high-quality MAGs (>75% completeness, <5% contamination) harboring *nosZ* genes was recovered from the 16 metagenome datasets generated from the N_2O-reducing microcosms (Fig. 3A, Supplementary Tables S8 and S9). Eight of these 17 MAGs have high relative abundance (TAD80 > 1%) in the corresponding metagenomes, revealing that these MAGs represented abundant members of the enriched communities (Fig. 3B). Only five MAGs with *nosZ* were detected in the metagenomic data of the original soils with relative abundance of ranging between 0.01% and 0.02% (Supplementary Fig. S9), much lower than the relative abundances observed in the corresponding microcosms (Fig. 3B). The relative abundance of MAGs derived from acidic microcosms in the corresponding (i.e. same soil sample) circumneutral microcosms was negligible, as was the relative abundance of MAGs derived from circumneutral microcosms in the corresponding acidic microcosms (Supplementary Fig. S10). This observation indicates the strong impact of pH on the enrichment of N_2O-reducers in microcosms that received N_2O.

The AAI results assigned all 17 MAGs harboring *nosZ* genes to novel taxa (Supplementary Table S10), indicating an unexplored diversity of N_2O reducers exists in the tropical forest soils and can be enriched in the N_2O-reducing microcosms. Six of eight MAGs recovered from acidic N_2O-reducing microcosms were assigned to the genera *Desulfitobacterium*, *Rhodoplanes*, *and Desulfosporosinus* with AAI values exceeding 68% (Supplementary Table S10), probably representing novel species [66]. The AAI similarities between the remaining two MAGs, PE_pH4.5_10_MAG7 and MAG8, and the corresponding closest relatives are 45.04% and 44.04%, respectively, suggesting these MAGs represent novel families (Fig. 3A and Supplementary Table S10). MAGs obtained from circumneutral, N_2O-reducing microcosms were taxonomically related to the genera *Azospira*, *Sulfurimicrobium*, *Dechloromonas*, and *Desulfitobacterium* (Supplementary Table S10).

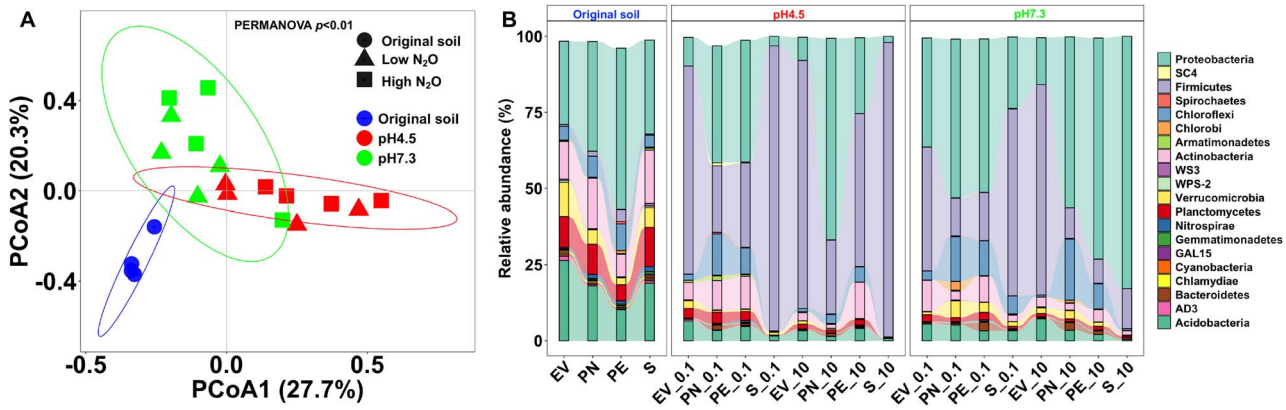

Figure 1. Microbial community composition of the original tropical forest soils and the N_2O-reducing microcosms maintained under low versus high levels of N_2O and at pH 4.5 versus pH 7.3; (A) beta diversity of microbial communities based on weighted Unifrac analysis of 16S rRNA gene fragments recovered from the metagenomes; samples are visualized by PCoA with colors distinguishing original soils and microcosms at acidic versus circumneutral pH; the ellipses represent the 95% confidence intervals; (B) the relative abundance distributions of the top 20 phyla observed in the original soils and the different microcosms; the numerals shown on the x-axis labels indicate the volumes of N_2O added with each feeding to the microcosms (0.1 ml [0.02 mM aqueous N_2O] versus 10 ml [2 mM aqueous N_2O]).

Functional analysis of MAGs harboring *nosZ* genes

Key metabolic pathways or functions of the 17 MAGs harboring *nosZ* were predicted based on KEGG annotation (Fig. 3C). All eight MAGs obtained from acidic N_2O-reducing microcosms lack the hallmark denitrification genes *nirK/nirS*, which encode nitrite reductase. This indicates that these organisms are non-denitrifiers. In contrast, seven of the nine MAGs derived from circumneutral microcosms carried a complete set of genes, including *nirS*, for canonical denitrification (i.e. $NO_3^- \rightarrow NO_2^- \rightarrow N_2O \rightarrow N_2$). In addition to *nosZ*, other genes of the *nos* cluster were detected in all MAGs (Supplementary Fig. S11). These findings indicate that non-denitrifying N_2O-reducing bacteria may be the main drivers for N_2O reduction in low pH soils. NosZ is a copper-containing enzyme and the extracellular copper concentration controls *nosZ* expression [67]. Notably, genes for copper transport were identified in 14 of the 17 MAGs harboring *nosZ*. Sources of electrons for reductive processes, such as N_2O reduction, were exogenously added lactate and organic material associated with the soil. Lactate was readily consumed in all live microcosms. The analysis of PE_pH4.5_10_MAG6 and MAG7 recovered from acidic N_2O-reducing microcosms revealed genes encoding L-lactate dehydrogenase (*LDH*, K00016), which are implicated in the conversion of lactate to pyruvate. Only PE_pH4.5_10_MAG6 contained the complete set of genes (*pta*, K13788, and *acyP*, K01512) required to metabolize lactate to acetate (Fig. 3C). In addition, five MAGs, three from acidic and two from circumneutral pH microcosms, possessed genes implicated in the fermentation of pyruvate to formate and acetyl-CoA (Fig. 3C). These findings suggest that most MAGs harboring *nosZ* genes were unable to directly utilize lactate as an electron donor. Collectively, these results demonstrate that MAGs harboring *nosZ* genes are taxonomically and metabolically diverse.

nosZ genes in metagenomes representing low pH soil biomes

A total of 27 metagenomes from low pH (pH 3.5–5.7) forest, agricultural, and permafrost soil ecosystems were analyzed (Supplementary Table S3), and all of them harbored *nosZ* sequences. *nosZ* abundances ranged from 0.002 ± 0.001 to 0.25 ± 0.11 genome equivalents (i.e. the fraction of genomes expected to carry *nosZ* assuming one gene copy per genome; Fig. 4), suggesting that the respective acidic soils have N_2O reduction potential. The highest abundances of *nosZ* genes were observed in the permafrost soil, and the lowest abundances were detected in two temperate forest soils. *nosZ* genes were also abundant in low pH tropical forest soils, which typically have high N_2 fixation and nitrogen turnover activities. An expanded survey that included the 27 metagenomic datasets from low pH plus eight datasets from pH 6 to 7.5 soils revealed that *nosZ* sequences representing low pH soil biomes were predominantly found in pH 4.5–6 environments (Supplementary Fig. S12). The number of metagenome datasets from acidic soils is currently limited; however, the observation that *nosZ* genes occur in all acidic soils included in the analysis suggests broad distribution of low pH microbial N_2O reduction potential.

Discussion

pH paradigm for microbial N_2O reduction

Biological N_2O reduction is catalyzed by microorganisms expressing NosZ with maximum efficiency observed at circumneutral pH [68, 69]. N_2O reduction under acidic pH conditions has received considerable attention; however, experimental work with laboratory cultures has indicated that NosZ activity ceases at pH <5.7 [18, 20, 27, 28]. These observations have been used to explain the lack of N_2O reduction activity under low pH conditions, and acidic environments are generally considered N_2O sources. NosZ is a periplasmic enzyme, and biochemical studies suggested that low pH impacts the assembly and maturation of functional NosZ [18], a plausible explanation for the observed lack of N_2O reduction activity at acidic pH. In contrast to the observations with laboratory cultures, soil microcosms studies reported N_2O reduction at pH <5.7 [70–72]. A possible reason for the contradictory findings is the presence of microsites within the soil matrix with higher pH than the measured bulk aqueous phase pH, allowing microbial N_2O reduction to occur in such micro-environments [18, 73, 74]. Further, the interpretation of observations made in short-term soil microcosm incubations is not straightforward because it is unclear if the N_2O reduction activity observed under acidic pH conditions is due to residual activity of existing biomass, or linked to the formation of new cells that conserve energy for growth from N_2O reduction. The sustainable reduction of N_2O

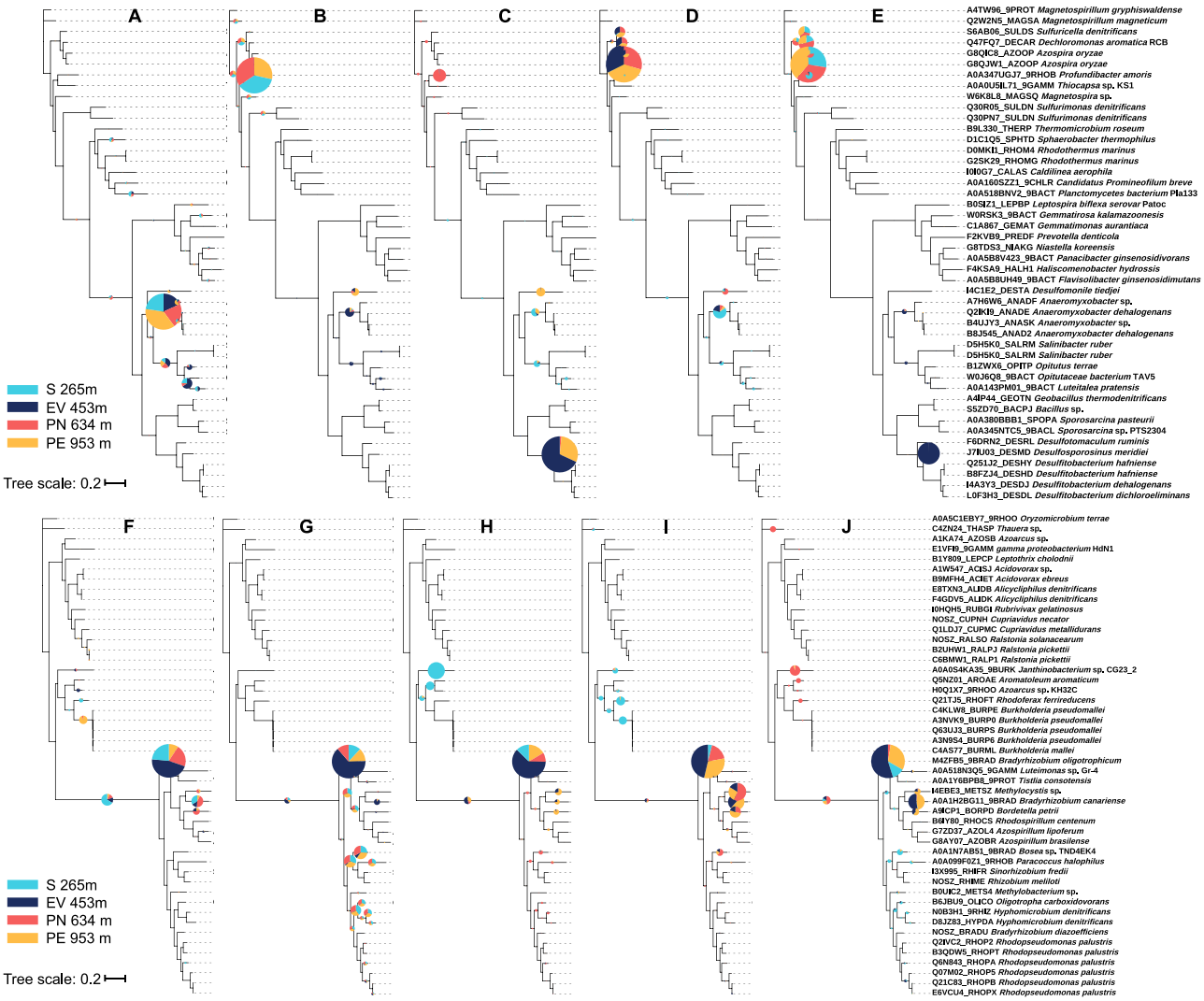

Figure 2. Phylogenetic diversity of *nosZ* reads recovered from the four original soils and the 16 microcosms maintained at pH 4.5 versus pH 7.3 and at low versus high levels of N_2O; trimmed Clade II and Clade I *nosZ* reads in the metagenomes were identified by ROCker and placed in the corresponding reference *nosZ* phylogenetic tree, as described in the Methods section; the radii of the pie charts are proportional to the number of reads assigned to each *nosZ* subclade and the colors represent the different soils; (A) diversity of Clade II *nosZ* reads from metagenomes of the four original soil samples; (B) phylogenetic information of Clade II *nosZ* in N_2O-reducing microcosms at acidic pH with low level of N_2O; phylogenetic information of Clade II *nosZ* in microcosms at acidic pH with high level of N_2O (C), at circumneutral pH with low level N_2O (D), and at circumneutral pH with high level N_2O (E); (F) diversity of Clade I *nosZ* reads from metagenomes of the four original soil samples; (G) phylogenetic information of Clade I *nosZ* in N_2O-reducing microcosms at acidic pH with low level of N_2O; phylogenetic information of Clade I *nosZ* in microcosms at acidic pH with high level of N_2O (H), at circumneutral pH with low level N_2O (I), and at circumneutral pH with high level N_2O (J).

requires the formation of new biomass (i.e. growth) under the prevailing environmental conditions. Laboratory studies with consortia that utilize the toxin vinyl chloride as respiratory electron acceptor illustrate this issue. Reductive dechlorination activity was observed at pH <5.5 [73]; however, this activity relied on existing biomass produced at circumneutral pH, and growth of vinyl chloride-respiring *Dehalococcoides mccartyi* strains did not occur at acidic pH, indicating that a sustainable process in acidic groundwater cannot be envisioned [73]. In analogy, it is uncertain if the results of short-term microcosm studies without repeated N_2O feedings generate meaningful information to predict *in situ* N_2O reduction activity in low pH soils. Further complicating data interpretation is the observation that common oxygen-respiring bacteria (e.g. members of the *Gemmatimonadaceae*) utilize N_2O as an electron sink following oxygen depletion; however, this process is uncoupled from growth and not sustained under anoxia [75, 76]. The LEF soil microcosms were incubated for 15 months, and repeated N_2O additions were consumed at accelerating rates, an observation inconsistent with the activity of residual (i.e. non-growing) biomass and indicative of respiratory N_2O utilization and growth of N_2O reducers at pH 4.5. Our observations challenge the notion that efficient N_2O reduction requires circumneutral pH and suggest that N_2O reduction can be sustained under acidic pH conditions.

Impact of enrichment on N_2O-reducing taxa

Prior metagenomic work demonstrated that soils collected at different locations (i.e. elevations) in the LEF share the predominant Clade II *nosZ* genes and implicated similar taxa in N_2O reduction [23]. Enrichment during the 15-month microcosm incubation revealed that different Clade II type N_2O reducers are responsible for N_2O reduction in the LEF soil samples collected at different elevations (Figs 2 and 3). For instance, the metagenome analysis of the original soils prior to enrichment implicated *Anaeromyxobacter* populations as predominant N_2O reducers (Fig. 2). N_2O reduction by *Anaeromyxobacter* at circumneutral pH

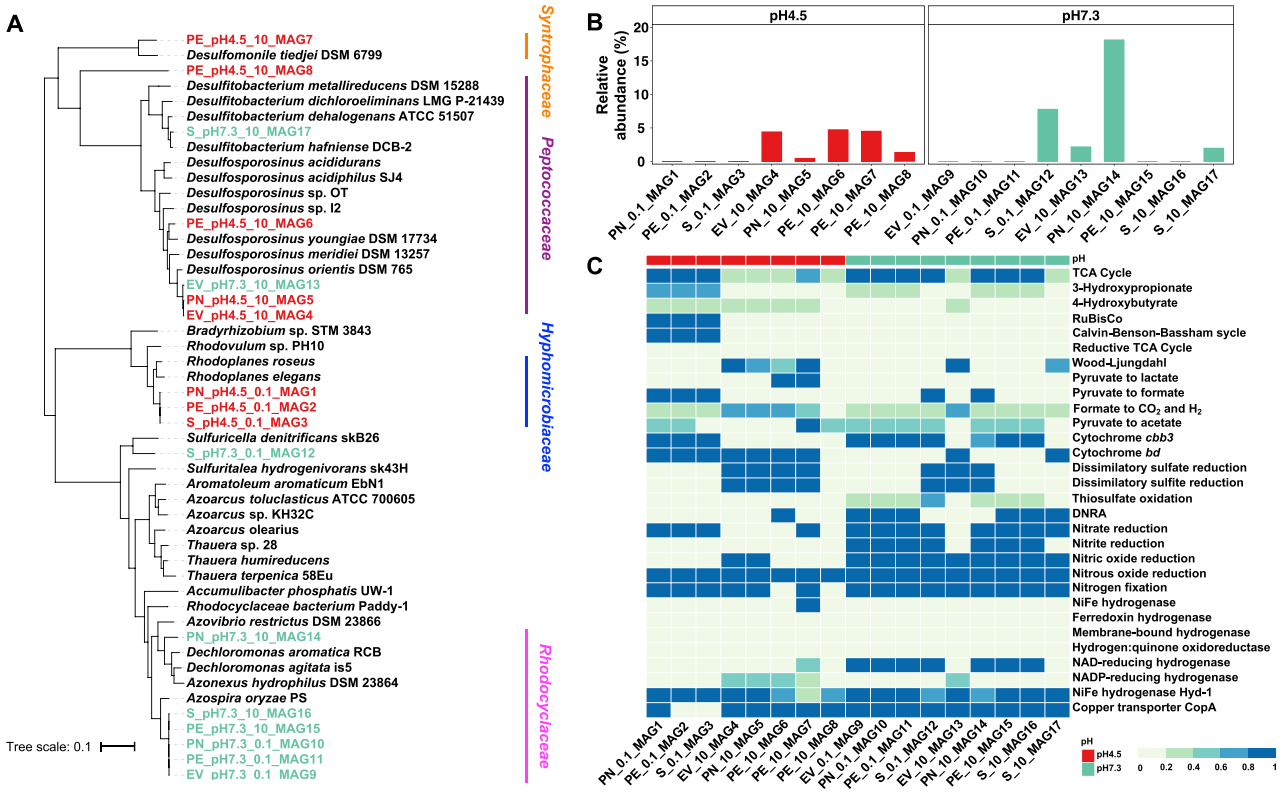

Figure 3. Phylogenetic and functional analysis of MAGs harboring *nosZ* genes; panel (A) shows a phylogenetic tree of the 17 MAGs harboring a *nosZ* gene and their closest neighbors based on the analysis of 120 bacterial marker genes; MAGs recovered from pH 4.5 and pH 7.3 N_2O-reducing microcosms are shown in red versus green font, respectively; panel (B) shows the relative abundance of each MAG harboring a *nosZ* gene in the corresponding N_2O-reducing microcosms; the relative abundance was calculated by normalizing TAD80 values to genome equivalents; the abundance of these MAGs in the original soil metagenomes was below 0.01% panel (C) depicts a heatmap showing the completeness of key metabolic pathways or functions in the 17 MAGs harboring a *nosZ* gene based on KEGG annotation; the numbers 0.1 and 10 in the x-axis labels represent the low and high levels of N_2O added to the microcosms, respectively.

has been demonstrated [6]; however, microcosms maintained at circumneutral pH selected for different N_2O-reducing taxa, including *Azospira* and *Dechloromonas* species, which have reported growth optima near pH 7.0 [77, 78]. Apparently, circumneutral pH favored *Azospira* and *Dechloromonas* over N_2O-reducing *Anaeromyxobacter* species in the laboratory microcosms. The relative abundance of *Anaeromyxobacter* sequences in the original soils can be explained by the presence of ferric iron, a favorable electron acceptor for *Anaeromyxobacter* [6]. In acidic N_2O-reducing microcosms, sequences representing the genera *Desulfosporosinus*, *Desulfitobacterium*, *Desulfomonile*, and *Rhodoplanes* increased. These genera comprise members that grow under acidic conditions (e.g. pH 4–6), and physiological and genomics investigations have shown that at least some species affiliated with these genera can reduce N_2O [79–82]. The tropical soil microcosm experiments demonstrate that pH selects for different N_2O-reducing taxa harboring Clade II *nosZ*, and show that N_2O reducers are distributed along the LEF elevational gradient spanning ~700 m. Despite the presence of taxa capable of low pH N_2O reduction, acidic tropical forest soils are considered N_2O emitters, raising the question of parameters, other than pH, that are limiting N_2O reduction activity in this relevant terrestrial ecosystem [18, 20, 24]. Our work focused on the roles of pH and N_2O concentration on the enrichment of N_2O-reducing taxa; a rigorous assessment of the overall community responses to pH and N_2O levels was not the goal, which would require more replication to enable robust statistics. The overall goal of this study was to evaluate whether enrichment conditions select for different N_2O-reducing taxa, and our current experimental approach achieves this goal by discovering that pH selects for different N_2O-reducing taxa in microcosms that stably reduce N_2O.

Non-denitrifying N_2O reducers responsible for N_2O reduction under low pH conditions

A recent metagenome analysis of the same LEF soils used for microcosm setup found abundant *nosZ* genes, with Clade II *nosZ* genes generally more abundant than Clade I *nosZ* genes [23]. Following the 15-month incubation period, Clade II *nosZ* dominated the *nosZ* gene pools in all microcosms irrespective of pH and N_2O concentration (Fig. 2 and Supplementary Fig. S7), indicating that the enrichment conditions favored populations with Clade II *nosZ*. The analysis of MAGs derived from acidic N_2O-reducing microcosms harboring *nosZ* indicated that non-denitrifiers (i.e. bacteria lacking *nirS*/*nirK*) representing novel taxa (Supplementary Table S10) are responsible for N_2O reduction (Fig. 3 and Supplementary Fig. S3). Prior studies reported that N_2O reduction under slightly acidic conditions (pH ~6.0) was driven by complete denitrifiers that represent cultivated taxa [83, 84]. Consistent with these prior reports, the MAGs with *nosZ* derived from microcosms maintained at circumneutral pH represent complete denitrifiers. Of note, three MAGs derived from acidic microcosms with low level of N_2O each harbored two *nosZ* genes, one Clade I and one Clade II, a genotype observed for few species of the class *Betaproteobacteria* capable of denitrification at circumneutral pH [85]. Collectively, the findings show that circumneutral pH selects for complete denitrifiers, whereas acidic pH selects for

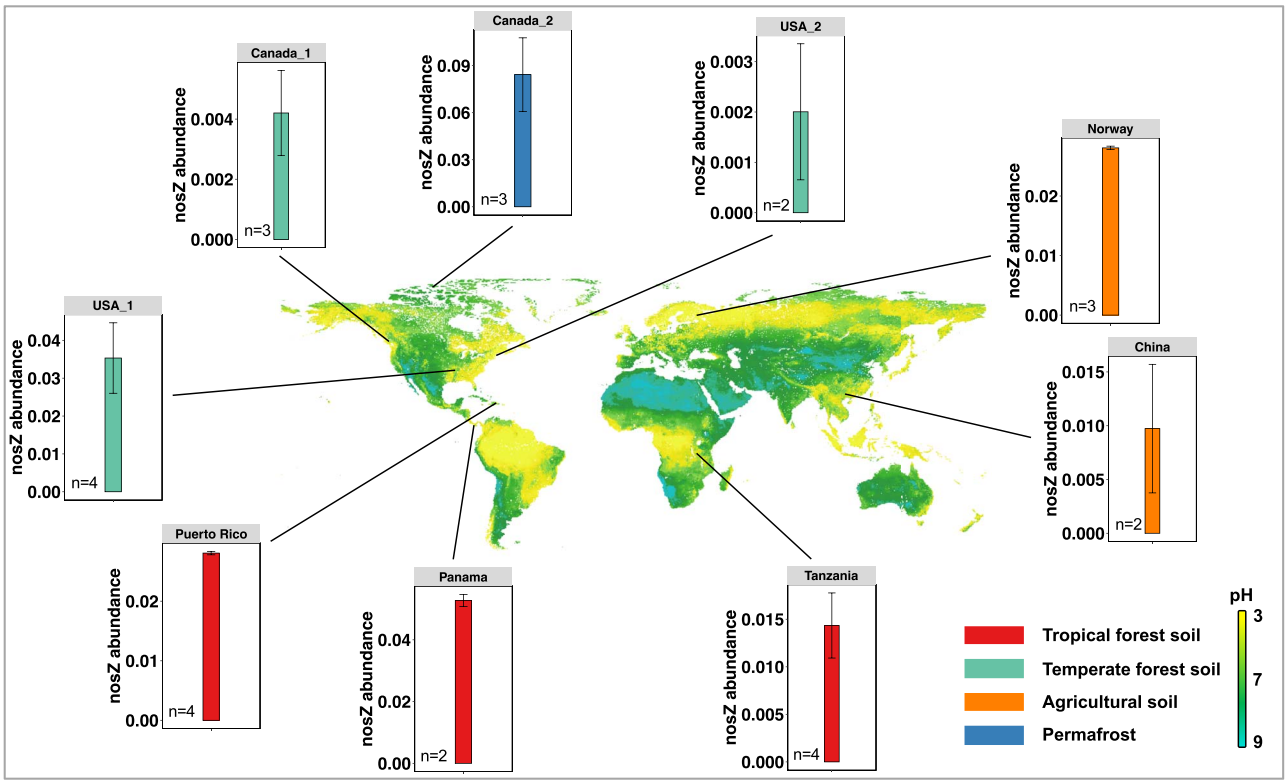

Figure 4. Distribution of N_2O reduction potential in acidic (pH 3.5–5.7) soils; detailed information about the metagenome datasets is provided in Supplementary Table S3; global soil pH data were obtained from the Soil Geographic Databases (https://www.isric.org); the plots show the total abundance of *nosZ* genes per genome equivalent; the black lines point to the approximate locations from where the soil metagenomes were derived.

non-denitrifying N_2O reducers in the tropical forest soils studied here. A relevant conclusion from this observation is that complete denitrifiers may not represent representative models to study low pH N_2O reduction.

Impact of N_2O concentration on N_2O reduction

A striking difference in microcosms with 0.02 mM versus 2 mM N_2O was the extended lag phase observed in the high-level N_2O microcosms independent of the pH condition. A possible explanation for the delayed start of N_2O consumption is the inhibition of corrinoid-dependent pathways. Micromolar concentrations of N_2O were shown to repress methionine biosynthesis [67], methanogenesis [86], methylmercury formation [87], and bacterial reductive dechlorination [32], all processes that involve enzymatic steps that strictly depend on the cobalt (I) supernucleophile, a species highly susceptible to oxidation by N_2O [88]. An initial N_2O concentration of 2 mM exceeds the reported inhibitory constants for corrinoid-dependent enzymes about 100-fold, suggesting the disruption of metabolic pathways directly or indirectly impacted N_2O-consuming populations. Only a subset of bacteria and archaea synthesize corrinoids [89], and corrinoid prototrophs supply this essential nutrient to corrinoid auxotrophs [90, 91]. The addition of N_2O disrupts these microbe–microbe interactions, which are influenced by the concentration of N_2O. Also possible is that the delayed onset of N_2O reduction in microcosms with high level of N_2O reflects a switch to corrinoid-independent metabolic pathways [32, 67].

Implications for N_2O reduction in low pH environments

Global atmospheric N_2O concentrations are on the rise, and the acidification of agricultural and forest soils, two major sources of atmospheric N_2O, is predicted to exacerbate emissions [4, 92, 93]. Soils with a pH below 5.5 currently comprise ~30% of the global ice-free land area and are mainly distributed in the northern temperate to cold belt and the southern tropical belt [94]. Our findings suggest that yet-to-be characterized, non-denitrifying bacterial taxa catalyze N_2O reduction at acidic pH. The microbial N_2O reduction potential appears to be distributed in acidic soils (Fig. 4), a finding likely to be substantiated as more metagenomes representing low pH microbiomes become available. These observations seem at odds with the dogma that acidic environmental systems are predominantly N_2O sources, and future research should address two major knowledge gaps. Although N_2O pools (i.e. how much is there?) can be quantitatively captured, robust tools to measure N_2O fluxes (i.e. the rates of N_2O formation and consumption) that ultimately determine emissions are lacking. Thus, it is not obvious if N_2O emissions from acidic soil ecosystems reflect a lack of microbial N_2O consumption capacity or an imbalance between N_2O formation versus consumption. Very limited information is available about the taxonomic diversity, physiology, and ecology of microbes that reduce N_2O under acidic conditions. This study identified several genera (i.e. *Desulfosporosinus*, *Desulfitobacterium*, *Desulfomonile*, and *Rhodoplanes*) as potential targets for more detailed exploration of low pH N_2O reduction, and future efforts should focus on the isolation and characterization of N_2O reducers from low pH environments to generate detailed process understanding.

Author contributions

Yanchen Sun, Yongchao Yin, and Frank E. Löffler conceptualized the research and designed experiments. Frank E. Löffler, Héctor L. Ayala-del-Río, and Grizelle González collected soil samples.,

Yanchen Sun and Yongchao Yin performed microcosm experiments and analytical work. Yanchen Sun conducted DNA extraction and bioinformatic analyses with help from Yongchao Yin, Guang He, Gyuhyon Cha, and Konstantinos T. Konstantinidis. Yanchen Sun and Frank E. Löffler wrote the manuscript with input from all coauthors.

Supplementary material

Supplementary material is available at *ISME Communications* online.

Conflict of interest

The authors declare no competing interest.

Funding

The authors acknowledge funding through the Dimensions of Biodiversity program of the US National Science Foundation (awards 1831582 to K.T.K. and 1831599 to F.E.L.). Y.S., Y.Y., and G.H. acknowledge the support from the China Scholarship Council.

Data availability

All metagenomic datasets were deposited in the European Nucleotide Archive under project PRJNA901179, and their respective accession numbers can be found in the Supplementary Table S2. The detail information of metagenomic data derived from low pH and circumneutral soils are summarized in Supplementary Table S3. Scripts for bioinformatics pipeline and statistical analyses are available upon request.

References

1. Houghton JT. *Climate change 1995: the science of climate change: contribution of working group I to the second assessment report of the intergovernmental panel on climate change*. Cambridge University Press, Cambridge 1996.
2. Ravishankara A, Daniel JS, Portmann RW. Nitrous oxide (N_2O): the dominant ozone-depleting substance emitted in the 21st century. *Science* 2009;**326**:123–5. https://doi.org/10.1126/science.1176985
3. Prinn RG, Weiss RF, Arduini J *et al.* History of chemically and radiatively important atmospheric gases from the advanced global atmospheric gases experiment (AGAGE). *Earth Syst Sci Data* 2018;**10**:985–1018. https://doi.org/10.5194/essd-10-985-2018
4. Tian H, Xu R, Canadell JG *et al.* A comprehensive quantification of global nitrous oxide sources and sinks. *Nature* 2020;**586**:248–56. https://doi.org/10.1038/s41586-020-2780-0
5. Knowles R. Denitrification. *Microbiol Rev* 1982;**46**:43–70. https://doi.org/10.1128/mr.46.1.43-70.1982
6. Onley JR, Ahsan S, Sanford RA *et al.* Denitrification by *Anaeromyxobacter dehalogenans*, a common soil bacterium lacking the nitrite reductase genes *nirS* and *nirK*. *Appl Environ Microbiol* 2018;**84**:e01985–17. https://doi.org/10.1128/AEM.01985-17
7. Bremner J, Blackmer AM. Nitrous oxide: emission from soils during nitrification of fertilizer nitrogen. *Science* 1978;**199**:295–6. https://doi.org/10.1126/science.199.4326.295
8. Sun Y, De Vos P, Willems A. Influence of nitrate and nitrite concentration on N_2O production via dissimilatory nitrate/nitrite reduction to ammonium in *Bacillus paralicheniformis* LMG 6934. *Microbiology* 2018;**7**:e00592. https://doi.org/10.1002/mbo3.592
9. Sanford RA, Wagner DD, Wu Q *et al.* Unexpected nondenitrifier nitrous oxide reductase gene diversity and abundance in soils. *Proc Natl Acad Sci USA* 2012;**109**:19709–14. https://doi.org/10.1073/pnas.1211238109
10. Jones CM, Graf DR, Bru D *et al.* The unaccounted yet abundant nitrous oxide-reducing microbial community: a potential nitrous oxide sink. *ISME J* 2013;**7**:417–26. https://doi.org/10.1038/ismej.2012.125
11. Shan J, Sanford RA, Chee-Sanford J *et al.* Beyond denitrification: the role of microbial diversity in controlling nitrous oxide reduction and soil nitrous oxide emissions. *Glob Chang Biol* 2021;**27**:2669–83. https://doi.org/10.1111/gcb.15545
12. Orellana L, Rodriguez-R L, Higgins S *et al.* Detecting nitrous oxide reductase (*nosZ*) genes in soil metagenomes: method development and implications for the nitrogen cycle. *mBio* 2014;**5**:10–1128. https://doi.org/10.1128/mBio.01193-14
13. Domeignoz-Horta LA, Putz M, Spor A *et al.* Non-denitrifying nitrous oxide-reducing bacteria-an effective N_2O sink in soil. *Soil Biol Biochem* 2016;**103**:376–9. https://doi.org/10.1016/j.soilbio.2016.09.010
14. Yoon S, Nissen S, Park D *et al.* Nitrous oxide reduction kinetics distinguish bacteria harboring Clade I NosZ from those harboring Clade II NosZ. *Appl Environ Microbiol* 2016;**82**:3793–800. https://doi.org/10.1128/AEM.00409-16
15. Čuhel J, Šimek M, Laughlin RJ *et al.* Insights into the effect of soil pH on N_2O and N_2 emissions and denitrifier community size and activity. *Appl Environ Microbiol* 2010;**76**:1870–8. https://doi.org/10.1128/AEM.02484-09
16. Suenaga T, Riya S, Hosomi M *et al.* Biokinetic characterization and activities of N_2O-reducing bacteria in response to various oxygen levels. *Front Microbiol* 2018;**9**:697. https://doi.org/10.3389/fmicb.2018.00697
17. Yoon S, Cruz-García C, Sanford R *et al.* Denitrification versus respiratory ammonification: environmental controls of two competing dissimilatory NO_3^-/NO_2^- reduction pathways in *Shewanella loihica* strain PV-4. *ISME J* 2015;**9**:1093–104. https://doi.org/10.1038/ismej.2014.201
18. Liu B, Frostegård Å, Bakken LR. Impaired reduction of N_2O to N_2 in acid soils is due to a posttranscriptional interference with the expression of *nosZ*. *mBio* 2014;**5**:e01383–14. https://doi.org/10.1128/mBio.01383-14
19. Van Den Heuvel R, Van Der Biezen E, Jetten M *et al.* Denitrification at pH 4 by a soil-derived *Rhodanobacter*-dominated community. *Environ Microbiol* 2010;**12**:3264–71. https://doi.org/10.1111/j.1462-2920.2010.02301.x
20. Frostegård Å, Vick SH, Lim NY *et al.* Linking meta-omics to the kinetics of denitrification intermediates reveals pH-dependent causes of N_2O emissions and nitrite accumulation in soil. *ISME J* 2022;**16**:26–37. https://doi.org/10.1038/s41396-021-01045-2
21. Werner C, Butterbach-Bahl K, Haas E *et al.* A global inventory of N_2O emissions from tropical rainforest soils using a detailed biogeochemical model. *Glob Biogeochem Cycles* 2007;**21**:21. https://doi.org/10.1029/2006GB002909
22. Tian H, Yang J, Xu R *et al.* Global soil nitrous oxide emissions since the preindustrial era estimated by an ensemble of terrestrial biosphere models: magnitude, attribution, and uncertainty. *Glob Chang Biol* 2019;**25**:640–59. https://doi.org/10.1111/gcb.14514
23. Karthikeyan S, Orellana LH, Johnston ER *et al.* Metagenomic characterization of soil microbial communities in the Luquillo experimental forest (Puerto Rico) and implications for nitrogen

cycling. *Appl Environ Microbiol* 2021;**87**:e00546–21. https://doi.org/10.1128/AEM.00546-21
24. Gallarotti N, Barthel M, Verhoeven E *et al.* In-depth analysis of N_2O fluxes in tropical forest soils of the Congo Basin combining isotope and functional gene analysis. *ISME J* 2021;**15**:3357–74. https://doi.org/10.1038/s41396-021-01004-x
25. Houlton BZ, Wang Y-P, Vitousek PM *et al.* A unifying framework for dinitrogen fixation in the terrestrial biosphere. *Nature* 2008;**454**:327–30. https://doi.org/10.1038/nature07028
26. Dalal RC, Wang W, Robertson GP *et al.* Nitrous oxide emission from Australian agricultural lands and mitigation options: a review. *Soil Res* 2003;**41**:165–95. https://doi.org/10.1071/SR02064
27. Wang Y, Guo J, Vogt RD *et al.* Soil pH as the chief modifier for regional nitrous oxide emissions: new evidence and implications for global estimates and mitigation. *Glob Chang Biol* 2018;**24**:e617–26. https://doi.org/10.1111/gcb.13966
28. Bakken LR, Bergaust L, Liu B *et al.* Regulation of denitrification at the cellular level: a clue to the understanding of N_2O emissions from soils. *Philos Trans R Soc* 2012;**367**:1226–34. https://doi.org/10.1098/rstb.2011.0321
29. Gould W, González G, Carrero RG. Structure and composition of vegetation along an elevational gradient in Puerto Rico. *J Veg Sci* 2006;**17**:653–64. https://doi.org/10.1111/j.1654-1103.2006.tb02489.x
30. Ping C-L, Michaelson GJ, Stiles CA *et al.* Soil characteristics, carbon stores, and nutrient distribution in eight forest types along an elevation gradient, eastern Puerto Rico. *Ecol Bull* 2013;**54**:67–86
31. Löffler FE, Sanford RA, Ritalahti KM. Enrichment, cultivation, and detection of reductively dechlorinating bacteria. *Meth Enzymol* 2005;**397**:77–111
32. Yin Y, Yan J, Chen G *et al.* Nitrous oxide is a potent inhibitor of bacterial reductive dechlorination. *Environ Sci Technol* 2018;**53**:692–701. https://doi.org/10.1021/acs.est.8b05871
33. Sander R. *Compilation of Henry's law constants for inorganic and organic species of potential importance in environmental chemistry*. Germany: Max-Planck Institute of Chemistry, Air Chemistry Department Mainz, 1999
34. Bolger AM, Lohse M, Usadel B. Trimmomatic: a flexible trimmer for Illumina sequence data. *Bioinformatics* 2014;**30**:2114–20. https://doi.org/10.1093/bioinformatics/btu170
35. Peng Y, Leung HC, Yiu S-M *et al.* IDBA-UD: a de novo assembler for single-cell and metagenomic sequencing data with highly uneven depth. *Bioinformatics* 2012;**28**:1420–8. https://doi.org/10.1093/bioinformatics/bts174
36. Wu Y-W, Simmons BA, Singer SW. MaxBin 2.0: an automated binning algorithm to recover genomes from multiple metagenomic datasets. *Bioinformatics* 2016;**32**:605–7. https://doi.org/10.1093/bioinformatics/btv638
37. Olm MR, Brown CT, Brooks B *et al.* dRep: a tool for fast and accurate genomic comparisons that enables improved genome recovery from metagenomes through de-replication. *ISME J* 2017;**11**:2864–8. https://doi.org/10.1038/ismej.2017.126
38. Parks DH, Imelfort M, Skennerton CT *et al.* CheckM: assessing the quality of microbial genomes recovered from isolates, single cells, and metagenomes. *Genome Res* 2015;**25**:1043–55. https://doi.org/10.1101/gr.186072.114
39. Rodriguez-R LM, Konstantinidis KT. The enveomics collection: a toolbox for specialized analyses of microbial genomes and metagenomes. *PeerJ Preprints* 2016;**4**:e1900v1. https://doi.org/10.7287/peerj.preprints.1900v1
40. Langmead B, Salzberg SL. Fast gapped-read alignment with Bowtie 2. *Nat Methods* 2012;**9**:357–9. https://doi.org/10.1038/nmeth.1923
41. Quinlan AR, Hall IM. BEDTools: a flexible suite of utilities for comparing genomic features. *Bioinformatics* 2010;**26**:841–2. https://doi.org/10.1093/bioinformatics/btq033
42. Royer C, Patin N, Jesser K *et al.* Comparison of metagenomic and traditional methods for diagnosis of *E. coli* enteric infections. *mBio* 2024;**15**:e03422–3. https://doi.org/10.1128/mbio.03422-23
43. Nayfach S, Pollard KS. Average genome size estimation improves comparative metagenomics and sheds light on the functional ecology of the human microbiome. *Genome Biol* 2015;**16**:51–18. https://doi.org/10.1186/s13059-015-0611-7
44. Boyd JA, Woodcroft BJ, Tyson GW. GraftM: a tool for scalable, phylogenetically informed classification of genes within metagenomes. *Nucleic Acids Res* 2018;**46**:e59–9. https://doi.org/10.1093/nar/gky174
45. McDonald D, Price MN, Goodrich J *et al.* An improved Greengenes taxonomy with explicit ranks for ecological and evolutionary analyses of bacteria and archaea. *ISME J* 2012;**6**:610–8. https://doi.org/10.1038/ismej.2011.139
46. Orellana LH, Rodriguez-R LM, Konstantinidis KT. ROCker: accurate detection and quantification of target genes in short-read metagenomic data sets by modeling sliding-window bitscores. *Nucleic Acids Res* 2017;**45**:gkw900–e14. https://doi.org/10.1093/nar/gkw900
47. Buchfink B, Reuter K, Drost H-G. Sensitive protein alignments at tree-of-life scale using DIAMOND. *Nat Methods* 2021;**18**:366–8. https://doi.org/10.1038/s41592-021-01101-x
48. Cha G, Meinhardt KA, Orellana LH *et al.* The influence of alfalfa-switchgrass intercropping on microbial community structure and function. *Environ Microbiol* 2021;**23**:6828–43. https://doi.org/10.1111/1462-2920.15785
49. Fish JA, Chai B, Wang Q *et al.* FunGene: the functional gene pipeline and repository. *Front Microbiol* 2013;**4**:291. https://doi.org/10.3389/fmicb.2013.00291
50. Eddy SR. Accelerated profile HMM searches. *PLoS Comput Biol* 2011;**7**:e1002195. https://doi.org/10.1371/journal.pcbi.1002195
51. Sievers F, Wilm A, Dineen D *et al.* Fast, scalable generation of high-quality protein multiple sequence alignments using Clustal omega. *Mol Syst Biol* 2011;**7**:539. https://doi.org/10.1038/msb.2011.75
52. Stamatakis A. RAxML version 8: a tool for phylogenetic analysis and post-analysis of large phylogenies. *Bioinformatics* 2014;**30**:1312–3. https://doi.org/10.1093/bioinformatics/btu033
53. Zhu W, Lomsadze A, Borodovsky M. *Ab initio* gene identification in metagenomic sequences. *Nucleic Acids Res* 2010;**38**:e132–2. https://doi.org/10.1093/nar/gkq275
54. Katoh K, Misawa K, Ki K *et al.* MAFFT: a novel method for rapid multiple sequence alignment based on fast Fourier transform. *Nucleic Acids Res* 2002;**30**:3059–66. https://doi.org/10.1093/nar/gkf436
55. Letunic I, Bork P. Interactive tree of life (iTOL) v3: an online tool for the display and annotation of phylogenetic and other trees. *Nucleic Acids Res* 2016;**44**:W242–5. https://doi.org/10.1093/nar/gkw290
56. Chaumeil P-A, Mussig AJ, Hugenholtz P *et al.* GTDB-Tk: a toolkit to classify genomes with the genome taxonomy database. *Bioinformatics* 2020;**36**:1925–7. https://doi.org/10.1093/bioinformatics/btz848
57. Parks DH, Chuvochina M, Chaumeil P-A *et al.* A complete domain-to-species taxonomy for bacteria and archaea. *Nat Biotechnol* 2020;**38**:1079–86. https://doi.org/10.1038/s41587-020-0501-8
58. Meziti A, Rodriguez-R LM, Hatt JK *et al.* The reliability of metagenome-assembled genomes (MAGs) in representing natural populations: insights from comparing MAGs against isolate

genomes derived from the same fecal sample. *Appl Environ Microbiol* 2021;**87**:e02593–20. https://doi.org/10.1128/AEM.02593-20
59. Hyatt D, Chen G-L, LoCascio PF *et al.* Prodigal: prokaryotic gene recognition and translation initiation site identification. *BMC Bioinformatics* 2010;**11**:1–11. https://doi.org/10.1186/1471-2105-11-119
60. Aramaki T, Blanc-Mathieu R, Endo H *et al.* KofamKOALA: KEGG ortholog assignment based on profile HMM and adaptive score threshold. *Bioinformatics* 2020;**36**:2251–2. https://doi.org/10.1093/bioinformatics/btz859
61. Graham E, Heidelberg J, Tully B. Potential for primary productivity in a globally-distributed bacterial phototroph. *ISME J* 2018;**12**:1861–6. https://doi.org/10.1038/s41396-018-0091-3
62. Price MN, Dehal PS, Arkin AP. FastTree 2–approximately maximum-likelihood trees for large alignments. *PLoS One* 2010;**5**:e9490. https://doi.org/10.1371/journal.pone.0009490
63. Gómez-Rubio V. ggplot2-elegant graphics for data analysis. *J Stat Softw* 2017;**77**:1–3. https://doi.org/10.18637/jss.v077.b02
64. McMurdie PJ, Holmes S. Phyloseq: an R package for reproducible interactive analysis and graphics of microbiome census data. *PLoS One* 2013;**8**:e61217. https://doi.org/10.1371/journal.pone.0061217
65. Oksanen J, Blanchet FG, Kindt R *et al. Package 'vegan'. Community ecology package, version 2. The comprehensive R archive network (CRAN)* 2013.
66. Konstantinidis KT, Rosselló-Móra R, Amann R. Uncultivated microbes in need of their own taxonomy. *ISME J* 2017;**11**:2399–406. https://doi.org/10.1038/ismej.2017.113
67. Sullivan MJ, Gates AJ, Appia-Ayme C *et al.* Copper control of bacterial nitrous oxide emission and its impact on vitamin B_{12}-dependent metabolism. *Proc Natl Acad Sci USA* 2013;**110**:19926–31. https://doi.org/10.1073/pnas.1314529110
68. Fujita K, Chan JM, Bollinger JA *et al.* Anaerobic purification, characterization and preliminary mechanistic study of recombinant nitrous oxide reductase from *Achromobacter cycloclastes*. *J Inorg Biochem* 2007;**101**:1836–44. https://doi.org/10.1016/j.jinorgbio.2007.06.029
69. Blum JM, Su Q, Ma Y *et al.* The pH dependency of N-converting enzymatic processes, pathways and microbes: effect on net N_2O production. *Environ Microbiol* 2018;**20**:1623–40. https://doi.org/10.1111/1462-2920.14063
70. Palmer K, Biasi C, Horn MA. Contrasting denitrifier communities relate to contrasting N_2O emission patterns from acidic peat soils in arctic tundra. *ISME J* 2012;**6**:1058–77. https://doi.org/10.1038/ismej.2011.172
71. Palmer K, Horn MA. Actinobacterial nitrate reducers and proteobacterial denitrifiers are abundant in N_2O-metabolizing palsa peat. *Appl Environ Microbiol* 2012;**78**:5584–96. https://doi.org/10.1128/AEM.00810-12
72. Lim NY, Frostegård Å, Bakken LR. Nitrite kinetics during anoxia: the role of abiotic reactions versus microbial reduction. *Soil Biol Biochem* 2018;**119**:203–9. https://doi.org/10.1016/j.soilbio.2018.01.006
73. Yang Y, Cápiro NL, Marcet TF *et al.* Organohalide respiration with chlorinated ethenes under low pH conditions. *Environ Sci Technol* 2017;**51**:8579–88. https://doi.org/10.1021/acs.est.7b01510
74. Alldredge AL, Cohen Y. Can microscale chemical patches persist in the sea? Microelectrode study of marine snow, fecal pellets. *Science* 1987;**235**:689–91. https://doi.org/10.1126/science.235.4789.689
75. Park D, Kim H, Yoon S. Nitrous oxide reduction by an obligate aerobic bacterium, *Gemmatimonas aurantiaca* strain T-27. *Appl Environ Microbiol* 2017;**83**:e00502–17. https://doi.org/10.1128/AEM.00502-17
76. Kellermann R, Hauge K, Tjåland R *et al.* Preparation for denitrification and phenotypic diversification at the cusp of anoxia: a purpose for N_2O reductase *Vis-à-Vis* multiple roles of O_2. *Appl Environ Microbiol* 2022;**88**:e01053–22. https://doi.org/10.1128/aem.01053-22
77. Reinhold-Hurek B, Hurek T. Reassessment of the taxonomic structure of the diazotrophic genus *Azoarcus sensu lato* and description of three new genera and new species, *Azovibrio restrictus* gen. nov., sp. nov., *Azospira oryzae* gen. nov., sp. nov. and *Azonexus fungiphilus* gen. nov., sp. nov. *Int J Syst Evol Microbiol* 2000;**50**:649–59. https://doi.org/10.1099/00207713-50-2-649
78. Han H, Song B, Song MJ *et al.* Enhanced nitrous oxide production in denitrifying *Dechloromonas aromatica* strain RCB under salt or alkaline stress conditions. *Front Microbiol* 2019;**10**:1203. https://doi.org/10.3389/fmicb.2019.01203
79. Villemur R, Lanthier M, Beaudet R *et al.* The *Desulfitobacterium* genus. *FEMS Microbiol Rev* 2006;**30**:706–33. https://doi.org/10.1111/j.1574-6976.2006.00029.x
80. Spring S, Rosenzweig F. The Genera *Desulfitobacterium* and *Desulfosporosinus*: taxonomy. In: Dworkin M, Falkow S, Rosenberg E, Schleifer KH, Stackebrandt E. (eds). *The Prokaryotes* 2016. Springer, New York, NY. https://doi.org/10.1007/0-387-30744-3_24
81. DeWeerd KA, Mandelco L, Tanner RS *et al. Desulfomonile tiedjei* gen. nov. and sp. nov., a novel anaerobic, dehalogenating, sulfate-reducing bacterium. *Arch Microbiol* 1990;**154**:23–30. https://doi.org/10.1007/BF00249173
82. Hiraishi A, Ueda Y. *Rhodoplanes* gen. nov., a new genus of phototrophic bacteria including *Rhodopseudomonas rosea* as *Rhodoplanes roseus* comb. nov. and *Rhodoplanes elegans* sp. nov. *Int J Syst Evol Microbiol* 1994;**44**:665–73. https://doi.org/10.1099/00207713-44-4-665
83. Lycus P, Bøthun KL, Bergaust L *et al.* Phenotypic and genotypic richness of denitrifiers revealed by a novel isolation strategy. *ISME J* 2017;**11**:2219–32. https://doi.org/10.1038/ismej.2017.82
84. Fukushi M, Mino S, Tanaka H *et al.* Biogeochemical implications of N_2O-reducing thermophilic *Campylobacteria* in deep-sea vent fields, and the description of *Nitratiruptor labii* sp. nov. *iScience* 2020;**23**:101462. https://doi.org/10.1016/j.isci.2020.101462
85. Semedo M, Wittorf L, Hallin S *et al.* Differential expression of Clade I and II N_2O reductase genes in denitrifying *Thauera linaloolentis* 47LolT under different nitrogen conditions. *FEMS Microbiol Lett* 2020;**367**:fnaa205. https://doi.org/10.1093/femsle/fnaa205
86. Klüber HD, Conrad R. Inhibitory effects of nitrate, nitrite, NO and N_2O on methanogenesis by *Methanosarcina barkeri* and *Methanobacterium bryantii*. *FEMS Microbiol* 1998;**25**:331–9. https://doi.org/10.1016/S0168-6496(97)00102-5
87. Zhang L, Yin Y, Sun Y *et al.* Inhibition of methylmercury and methane formation by nitrous oxide in Arctic tundra soil microcosms. *Environ Sci Technol* 2023;**57**:5655–65. https://doi.org/10.1021/acs.est.2c09457
88. Banks R, Henderson R, Pratt J. Reactions of gases in solution. Part III. Some reactions of nitrous oxide with transition-metal complexes. *J Chemi Soc A* 1968;2886–9. https://doi.org/10.1039/j19680002886
89. Shelton AN, Seth EC, Mok KC *et al.* Uneven distribution of cobamide biosynthesis and dependence in bacteria predicted

by comparative genomics. *ISME J* 2019;**13**:789–804. https://doi.org/10.1038/s41396-018-0304-9

90. Yan J, Şimşir B, Farmer AT *et al.* The corrinoid cofactor of reductive dehalogenases affects dechlorination rates and extents in organohalide-respiring *Dehalococcoides mccartyi*. *ISME J* 2016;**10**:1092–101. https://doi.org/10.1038/ismej.2015.197
91. Sokolovskaya OM, Shelton AN, Taga ME. Sharing vitamins: cobamides unveil microbial interactions. *Science* 2020;**369**:eaba0165. https://doi.org/10.1126/science.aba0165
92. Tian D, Niu S. A global analysis of soil acidification caused by nitrogen addition. *Environ Res Lett* 2015;**10**:024019. https://doi.org/10.1088/1748-9326/10/2/024019
93. Raut N, Dörsch P, Sitaula BK *et al.* Soil acidification by intensified crop production in South Asia results in higher $N_2O/(N_2 + N_2O)$ product ratios of denitrification. *Soil Biol Biochem* 2012;**55**:104–12. https://doi.org/10.1016/j.soilbio.2012.06.011
94. Von Uexküll H, Mutert E. Global extent, development and economic impact of acid soils. *Plant Soil* 1995;**171**:1–15. https://doi.org/10.1007/BF00009558